

Dual Contrastive Learning for General Face Forgery Detection

Ke Sun¹, Taiping Yao², Shen Chen², Shouhong Ding^{2*}, Jilin Li², Rongrong Ji^{1*}

¹Media Analytics and Computing Lab, Department of Artificial Intelligence,
School of Informatics, Xiamen University, 361005, China

²Youtu Lab, Tencent, China
skjack@stu.xmu.edu.cn, rrji@xmu.edu.cn
{taipingyao, kobeschen, ericshding, jerolinli}@tencent.com

Abstract

With various facial manipulation techniques arising, face forgery detection has drawn growing attention due to security concerns. Previous works always formulate face forgery detection as a classification problem based on cross-entropy loss, which emphasizes category-level differences rather than the essential discrepancies between real and fake faces, limiting model generalization in unseen domains. To address this issue, we propose a novel face forgery detection framework, named Dual Contrastive Learning (DCL), which specially constructs positive and negative paired data and performs designed contrastive learning at different granularities to learn generalized feature representation. Concretely, combined with the hard sample selection strategy, Inter-Instance Contrastive Learning (Inter-ICL) is first proposed to promote task-related discriminative features learning by especially constructing instance pairs. Moreover, to further explore the essential discrepancies, Intra-Instance Contrastive Learning (Intra-ICL) is introduced to focus on the local content inconsistencies prevalent in the forged faces by constructing local-region pairs inside instances. Extensive experiments and visualizations on several datasets demonstrate the generalization of our method against the state-of-the-art competitors.

1 Introduction

Over the past few years, face forgery methods have achieved significant success and received lots of attention in the computer vision community (Thies et al. 2015; Rossler et al. 2019; Dolhansky et al. 2020; Wang et al. 2020; Gu et al. 2021). As such techniques can generate high-quality fake videos that are even indistinguishable for human eyes, they can easily be abused by malicious users to cause severe societal problems or political threats. To mitigate such risks, it is of paramount importance to develop effective methods for detecting face forgery.

Early works (Afchar et al. 2018; Stehouwer et al. 2019; Dolhansky et al. 2020) treat face forgery detection as a binary classification problem and use the convolutional neural network (CNN) to distinguish the authenticity of the face. These methods achieve considerable performance in the intra-domain scenario, where the training and test sets manifest similar data distributions. However, faces in real

applications are varied from that in training set in terms of the camera type, pre-processing, compression rate, and attack method, *e.t.c.* These unseen domain gaps bring severe performance drops, thus limiting broader applications.

Recently, several works (Li et al. 2020; Sun et al. 2021; Liu et al. 2021a) are devoted to *general face forgery detection* (Sun et al. 2021) to relieve the generalizing problem. Face X-ray (Li et al. 2020) designs supervision named face X-ray, which focuses on the blending boundary induced by the image blending process. LTW (Sun et al. 2021) weights training samples via meta-learning. Besides, some attempt to obtain information from frequency domains, such as DCT (Qian et al. 2020), spatial-phase (Liu et al. 2021a) and SRM (Luo et al. 2021). However, these methods can be attributed to a binary classification network based on cross-entropy loss, which we argue is not suitable for general face forgery detection. Specifically, traditional cross-entropy based methods assume that all instances within each category should be close in feature distribution while ignoring the unique information of each sample. This information is proven in (Zhao et al. 2020) that could provide transferability knowledge for unseen forgery faces. Without additional constraints, a common cross-entropy classification framework is prone to overfitting on specific forged patterns (Luo et al. 2021). Moreover, the quality of forgery faces is different, and optimizing each sample equally as in the traditional framework makes it difficult to uncover the underlying forgery clues and is not conducive to generalization (Liu et al. 2021b; Sun et al. 2021). Therefore, a new framework is urgently needed to address the above issues.

In this paper, motivated by contrastive learning (He et al. 2020) that has been shown to outperform its supervised counterpart in transfer learning (Zhao et al. 2020), we propose a Dual Contrast Learning (DCL) framework for general facial forgery detection, as shown in Fig. 1. Since DCL requires two samples from different views of the same image as inputs, we first generate different data views as positive pairs via specially designed data transformations which can eliminate the task-independent information, such as background and face structure, *e.t.c.* Second, to preserve the instance transferability, we design the Inter-instance Contrastive Learning (Inter-ICL) to mine the association between instances. Specifically, Inter-ICL pulls the positive pairs closer together while pulling the true negatives of each

*Corresponding authors.

training instance away. The variance among instances can be preserved by alignment and uniformity (Wang and Isola 2020). We also propose a new hard sample selection strategy by comparing samples with their negative prototypes. This strategy can provide effective gradients to the contrastive loss and highlight samples with essential forgery clues. Third, considering the local inconsistencies prevalent in the forged faces, we design Intra-instance Contrastive Learning (Intra-ICL), which contrasts fake and real parts within forgery face to mine the general essential forgery clues.

- We propose a novel Dual Contrastive Learning (DCL) for general face forgery detection, which specially constructs positive and negative data pairs and performs contrastive learning at different granularities to further improve the generalization.
- We specially design Inter-Instance Contrastive Learning and Intra-Instance Contrastive Learning based on instance pairs among samples and local-region pairs within samples respectively to learn task-related essential features.
- Extensive experiments and visualizations demonstrate the effectiveness of our method against the state-of-the-art competitors.

2 Related Work

2.1 Face Forgery Detection

Face forgery detection is a classical problem in computer vision and graphics. Earlier studies focus on hand-crafted features such as eye blinking (Li, Chang, and Lyu 2018), inconsistent head poses (Yang, Li, and Lyu 2019) and visual artifacts (Matern, Riess, and Stamminger 2019). With the tremendous success of deep learning, convolutional neural network (CNN) is widely used to face forgery detection task and achieved better performance. For example, Stehouwer et al. (2019); Zhao et al. (2021) highlighted the manipulated regions via attention mechanism. Frank et al. (2020) first discovered the difference between real and forgery face under frequency domain. Subsequently, many works (Qian et al. 2020; Masi et al. 2020; Chen et al. 2021; Liu et al. 2021a) leverage frequency clues as the supplement to RGB information. Although the aforementioned methods achieve promising results in intra-domain where the data distributions in training set and test set are the same, the performance drops significantly when facing the unseen domain scenario.

Recently, some work focusing on general face forgery detection has been proposed. Face X-ray (Li et al. 2020) is supervised by the forged boundary that widely existed in blending operation. LTW (Sun et al. 2021) weight samples and provide gradient regularization via meta-learning. Luo et al. (2021) depress the texture bias via SRM operation to avoid overfitting on image content. However, these methods inherited from image classification models emphasize category-level differences rather than the essential discrepancies between real and fake images. To tackle these issues, we introduce dual-granularity contrastive learning framework to control the intra-class variance and preserve the transferability.

2.2 Supervised Contrastive Learning

Contrastive learning (He et al. 2020) has achieved great success in self-supervised representation. Khosla et al. (2020) extend it to the fully-supervised setting that can effectively leverage label information. The advantage of supervised contrastive learning (SCL) can be attributed twofold: Firstly, it can be used to change the feature distributions. Based on SCL, Bukchin et al. (2021) reduce the intra-class variance and eliminate the intra-class distinctions between subclasses in the coarse-to-fine few-shot task, while Wang et al. (2021) enforce pixel embeddings belonging to the same semantic class to be more similar than embeddings from different classes in semantic segmentation task. Secondly, SCL can eliminate the task-independent information by constructing positive data pairs. For example, Lo et al. (2021) decouple the correlation of the image scenes and illuminant via supervised contrastive learning for color constancy. Wang et al. (2021), focus on the 3D face presentation attack detection, learns discriminative features by comparing image pairs with diverse contexts. For face forgery detection, we leverage specially designed data transform methods as positive pairs and further boost the unseen domain performance via intra-instance contrastive learning and inter-instance contrastive learning.

3 Proposed Method

In this section, we introduce our Dual Contrastive Learning (DCL) framework for general face forgery detection, which simultaneous contrast features between different instances and within the instance. As shown in Fig 1, DCL trains the model via contrastive learning framework in a supervised manner. The beginning of the DCL is Data Views Generation (DVG) module to generate different views of inputs by special designed data augmentation, then features are extracted from the well-designed supervised contrastive learning architecture. Subsequently, the Inter-Instance Contrastive Learning module and Intra-Instance Contrastive Learning module are used to arrange the feature distribution and enhance the inconsistency of forgery faces, respectively.

3.1 Data Views Generation

In the contrastive learning framework (He et al. 2020), features are pulled closer if they are encoded views of the same image. Thus, it is important to generate different views as the positive pair. Traditional contrastive learning uses common data augmentation such as horizontal flip, random crop and gaussian blur to generate views. Different from the common classification task, the key of the general forgery face views’ generalization is to eliminate task-irrelevant contextual factors such as high-level face content, specific manipulated texture, background information *e.t.c.* Thus, we leverage the following specifically designed operations to generate different views: **1) RandomPatch.** To destroy the structure of the input face and highlight the focus on the forgery clues, we divide the input face into $k \times k$ patches, and then randomly shuffle them. **2) High-frequency enhancement.** Existing works (Fridrich and Kodovsky 2012) have proved

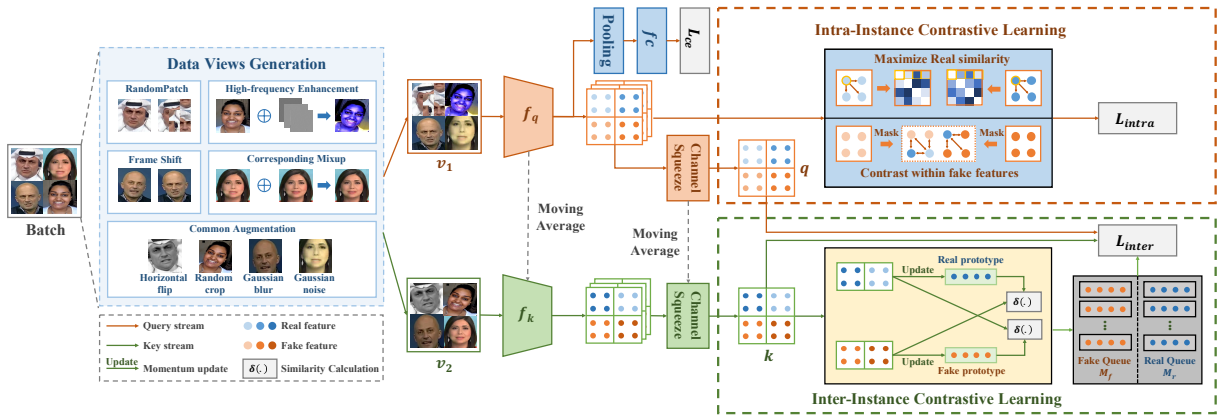


Figure 1: Overview of our proposed DCL framework. Given training images, we first transform them into two different views via the Data Views Generation module. Then the Intra-instance contrastive learning module and Inter-instance contrastive learning module are proposed to learn general features.

that the high-frequency features can help to boost the generalization ability. Take inspiration from it, we combine the SRM feature with the original image to enhance the high-frequency information. **3) Frame shift.** To reduce the influence of different expressions and motions on forged extraction, we choose different frames of the same video as different views. **4) Corresponding mixup.** In order to eliminate some obviously forgery clues and mine the essential features, we apply a mixup operation between fake images and its corresponding real images. Note that this operation is only used when the input is a fake image. All these methods are chosen with a certain probability and random combination becomes the final operations denoted as $v_1(\cdot)$ and $v_2(\cdot)$.

3.2 Architecture of Contrastive Learning

The input data $x_i \in \mathbb{R}^{H \times W \times 3}$ with label $y_i \in \{0, 1\}$ is firstly transformed into two different views $v_1(x_i)$ and $v_2(x_i)$ via data views generation module. Then two views are fed into CNN based query encoder f_q and key encoder f_k to obtain feature maps $f_q(v_1(x_i)) \in \mathbb{R}^{C \times H' \times W'}$ and $f_k(v_2(x_i)) \in \mathbb{R}^{C \times H' \times W'}$. Similar to the MoCo (He et al. 2020), the parameters of key encoder θ' is updated via exponential moving-average strategy from query encoder parameters θ :

$$\theta' = \beta\theta' + (1 - \beta)\theta, \quad (1)$$

where β is exponential hyper-parameter. Since it is important for face forgery detection task to locate the forgery clues in spatial dimensional, unlike traditional contrastive learning, we use spatial-wise instead of channel-wise features as contrastive objectives. Specifically, 1×1 convolution operation is applied to squeeze the channel dimensional to get query $q \in \mathbb{R}^{H' \times W'}$ and key $k \in \mathbb{R}^{H' \times W'}$. Subsequently, to perform classification and make full use of label information, a fully connected classifier f_c is inserted after query feature extraction. We formulated the binary cross-entropy loss L_{ce} as follows:

$$L_{ce} = y \log y' + (1 - y) \log(1 - y'), \quad (2)$$

where y' is the final predicted probability and y denoted the corresponding ground-truth label. During testing, only query encoder f_q and classifier f_c is used to get final prepositions.

3.3 Inter-Instance Contrastive Learning.

To preserve the instance discrimination of unique sample, we design an inter-instance contrastive learning module which pulls close the embedding of the different views of the same image and pull away the true negative samples on the hyperspherical plane.

Specifically, we maintain two feature queues: real queue M_r and fake queue M_f to construct the negative sample of the corresponding query. The normalized cosine similarity is used as the metric of features denoted as $\delta(u, v) = \frac{u \cdot v}{\|u\| \cdot \|v\|}$. Our inter-instance contrastive loss based upon the popular InfoNCE loss (Gutmann and Hyvärinen 2010) can be written as:

$$L_{inter} = -\log \frac{e^{\delta(q,k)/\tau}}{e^{\delta(q,k)/\tau} + \sum_{k_m \in K_q^-} e^{\delta(q,k_m)/\tau}}, \quad (3)$$

where τ is a temperature parameter which controls the scale of distribution. K_q^- represents the negative set of q , i.e. $K_q^- = M_f$ when q belongs to real, and $K_q^- = M_r$ when q belongs to fake. Unlike existing common supervised contrastive learning methods (Khosla et al. 2020) which maximizes the invariance among the same category views, L_{cl} only maximizes the invariance between two different views of single input, which decouples the impact of irrelevant forgery traces and does avoid the embedding instance of the same class in the proximity of one another. Thus, the variance of the intra-class distributions can be guaranteed so that more transferability knowledge is preserved.

Hard Sample Generation. Robinson et al. (2021); Wang et al. (2021) found that the hard negative pair selection is crucial for contrastive learning. Meanwhile, Sun et al. (2021) shows high-quality samples are more conducive to improving the generalization of the model. Thus, to bring

more gradient contributions for the L_{inter} and mine the essential general forgery features, we design a novel hard sample generation strategy to generate our feature queues M_f and M_r .

Our key idea can be derived as: *the more real the fake face is, the more it can be defined as a difficult sample*. Specifically, as shown in yellow dotted frame, we defined two prototypes P_{real} and P_{fake} for real and fake features respectively and updated using EMA scheme defined as:

$$P_{fake} = \alpha P_{fake} + (1 - \alpha) k_{fake}, \quad (4)$$

$$P_{real} = \alpha P_{real} + (1 - \alpha) k_{real}. \quad (5)$$

Then, we calculate the similarity of fake/fake feature and P_{real}/P_{fake} as the basis to decide whether the feature enqueue. More formally, the screening progress can be derived as:

$$\begin{cases} \delta(k_{fake}, P_{real}) > \theta, & M_f \leftarrow k_{fake} \\ \delta(k_{real}, P_{fake}) > \theta, & M_r \leftarrow k_{real}, \end{cases} \quad (6)$$

where θ is a threshold and the \leftarrow represents the enqueue operation. By doing this, the features in M_f and M_r of hard negatives have the following two properties: 1) their label is the same as the queue label. 2) it is hard for the model to distinguish their authenticity. 3) the quality of selected samples is higher. Thus, compared with ordinary feature queues without selection strategy, ours is more suitable for constructing true negative sample pairs.

3.4 Intra-Instance Contrastive Learning.

The aforementioned inter-instance contrastive learning module improves the generalization by contrastive among samples. To further promote generalized feature learning, we design an intra-instance contrastive learning module, which leverages the inconsistency of the forgery face by contrasting self-similarities within features.

Specifically, given forgery image x_{fi} , we first generate the pixel-level mask $m_i \in R^{H \times W}$ by subtracting its corresponding real image x_{ri} : $m_i = |x_i - x'_i|$. Then we resize the m_i into the same spatial size as the feature map $f_q(v_1(x_{fi}))$ denoted as $m'_i \in R^{H' \times W'}$. Subsequently, we segment the $f_q(v_1(x_{fi}))$ into real parts $P_r \in \{p_{r1}, p_{r2}, \dots, p_{rn}\}$ and forgery parts $P_f \in \{p_{f1}, p_{f2}, \dots, p_{fk}\}$ using m'_i , where $p_f, p_r \in R^C$ and n, k denote the number of real and fake parts thus $n + k = H'W'$. Then the intra-instance contrastive loss for forgery features L_{intra}^f is calculated based upon InfoNCE as follows:

$$L_{intra}^f = -\log \frac{\sum_{i,j=1}^n e^{\delta(p_{ri}, p_{rj})/\tau}}{\sum_{i,j=1}^n e^{\delta(p_{ri}, p_{rj})/\tau} + \sum_{i=1}^n \sum_{j=1}^k e^{\delta(p_{fi}, p_{rj})/\tau}}, \quad (7)$$

For real image x_{ri} , since all the features belongs to real, we expect for the self-similarity of $f_q(v_1(x_{ri}))$ become homogeneous. Thus, the intra-instance contrastive loss for real

features can be obtained by:

$$L_{intra}^r = -\log \text{sum}(e^{f_q(v_1(x_{ri})) \odot f_q(v_1(x_{ri}))'^T/\tau}), \quad (8)$$

where \odot represents the gram matrices multiplication and $\text{sum}(\cdot)$ represents the element-wise addition. T denote the transpose operation. The overall intra-instance contrastive loss L_{intra} within a batch can be derived as :

$$L_{intra} = L_{intra}^r + L_{intra}^f, \quad (9)$$

Different from (Chen et al. 2021) which directly use similarity pattern as features, our proposed intra-instance contrastive loss enhances the inconsistency of forgery face by pulling away the similarity of real and fake parts and depress the influence of forgery irrelevant information via pulling the real pairs closer. Note that L_{intra} do not aggregate the fake part together because we want to preserve the diversity of counterfeit traces.

3.5 Overall Loss Function

Considering both the cross-entropy loss based supervised learning branch and two InfoNCE losses based contrastive learning branches, the overall loss for our proposed method is:

$$L_{all} = \phi(L_{inter} + L_{intra}) + (1 - \phi)L_{ce}, \quad (10)$$

where ϕ is the hyper-parameters used to balance the cross-entropy loss and contrastive loss.

4 Experiments

4.1 Experimental Setting

Datasets. To evaluate our method, we conduct experiments on five famous challenging datasets: **FaceForensics++** (Rossler et al. 2019) is a large-scale forgery face dataset containing 720 videos for training and 280 videos for validation or testing. There are four different face synthesis approaches in FaceForensics++, including two deep leaning based methods (*DeepFakes* and *NeuralTextures*) and two graphics-based approaches (*Face2Face* and *FaceSwap*), which is suitable for conducting generalization experiments. The videos in FaceForensics++ have two kinds of video quality: high-quality (quantization parameter equal to 23) and low-quality (quantization parameter equal to 40). **Celeb-DF** (Li et al. 2019b) is another widely-used dataset, which contains 590 real videos and 5639 fake videos. Forgery videos are generated by face swap for each pair of the 59 subjects. **DFDC** (Dolhansky et al. 2020) is a large-scale deepfake datasets which contain 1133 real videos and 4080 fake videos with various manipulated methods. **DFD** is a Deepfake based dataset that has 363 real videos and 3068 fake videos. **Wild Deepfake** (Zi et al. 2020) is a recently released forgery face dataset contains 3805 real face sequences and 3509 fake face sequences. All the videos are obtained from the internet. Therefore, wild deepfake has a variety of synthesis methods and backgrounds, as well as character ids. We use DSFD (Li et al. 2019a) to extract faces for all datasets and randomly select 50 frames from each video for testing and training.

Method	FF++		DFD		DFDC		Wild Deepfake		Celeb-DF	
	AUC	EER	AUC	EER	AUC	EER	AUC	EER	AUC	EER
Xception	99.09	3.77	87.86	21.04	69.80	35.41	66.17	40.14	65.27	38.77
EN-b4	99.22	3.36	87.37	21.99	70.12	34.54	61.04	45.34	68.52	35.61
Face X-ray	87.40	-	85.60	-	70.00	-	-	-	74.20	-
MLDG	98.99	3.46	88.14	21.34	71.86	34.44	64.12	43.27	74.56	30.81
F3-Net	98.10	3.58	86.10	26.17	72.88	33.38	67.71	40.17	71.21	34.03
MAT(EN-b4)	99.27	3.35	87.58	21.73	67.34	38.31	70.15	36.53	76.65	32.83
GFF	98.36	3.85	85.51	25.64	71.58	34.77	66.51	41.52	75.31	32.48
LTW	99.17	3.32	88.56	20.57	74.58	33.81	67.12	39.22	77.14	29.34
Local-relation	99.46	3.01	89.24	20.32	76.53	32.41	68.76	37.50	78.26	29.67
Ours	99.30	3.26	91.66	16.63	76.71	31.97	71.14	36.17	82.30	26.53

Table 1: Cross-database evaluation from FF++(HQ) to DFD, DFDC, Wild Deepfake and Celeb-DF in terms of AUC and EER. The FF++ belongs to the intra-domain results while others represent to the unseen-domain.

Method	FF++	Celeb-DF
Meso-4	84.70	54.80
MesoInception4	83.00	53.60
FWA	80.10	56.90
Xception	95.50	65.50
Multi-task	76.30	54.30
SMIL	96.80	56.30
Two Branch	93.18	73.41
EN-b4	96.39	71.10
Multi-Attention	96.41	72.50
GFF	95.73	74.12
SPSL	96.91	76.88
Ours	96.97	81.00

Table 2: Cross-dataset evaluation from FF++(LQ) to deepfake class of FF++ and Celeb-DF in terms of AUC.

Implement details. We resize the input face into 299×299 , and use Adam optimizer to train the framework, where the weight decay is equal to $1e - 5$ with betas of 0.9 and 0.999. The learning rate is set to 0.001 and the batchsize is set to 32. The EfficientNet-b4 (Tan and Le 2019) pretrained on the ImageNet (Deng et al. 2009) is used as our encoders f_q and f_k . The exponential hyper-parameter β is set to 0.99. The temperature parameter τ of E.q. 3 is set to 0.07 and the query size $|M|$ is set to 30000. In addition, we set 0.9 and 0.5 for prototypes updating parameter α and threshold θ . For the balanced weight ϕ , we set $\phi = 0.1$ for the first 5 epochs as the warm-up period under the guidance of l_{ce} , then the ϕ is set to 0.5.

4.2 Quantitative Results

Cross-dataset evaluation. To demonstrate the generalization of DCL, we conduct extensive cross-dataset evaluations. Specifically, the models are trained on the FF++(HQ) and evaluated on the DFD, DFDC, Wild Deepfake, and

Train	Method	DF	F2F	FS	NT
DF	EN-b4	99.97	76.32	46.24	72.72
	MAT	99.92	75.23	40.61	71.08
	GFF	99.87	76.89	47.21	72.88
	Ours	99.98	77.13	61.01	75.01
F2F	EN-b4	84.52	99.20	58.14	63.71
	MAT	86.15	99.13	60.14	64.59
	GFF	89.23	99.10	61.30	64.77
	Ours	91.91	99.21	59.58	66.67
FS	EN-b4	69.25	67.69	99.89	48.61
	MAT	64.13	66.39	99.67	50.10
	GFF	70.21	68.72	99.85	49.91
	Ours	74.80	69.75	99.90	52.60
NT	EN-b4	85.99	48.86	73.05	98.25
	MAT	87.23	48.22	75.33	98.66
	GFF	88.49	49.81	74.31	98.77
	Ours	91.23	52.13	79.31	98.97

Table 3: Cross-manipulation evaluation in terms of AUC. Diagonal results indicate the intra-domain performance.

Celeb-DF, respectively. We compare DCL with several recently state-of-the-art methods, including **Xception** (Chollet 2017), **EfficientNet-b4** (Tan and Le 2019), **Face X-ray** (Tan and Le 2019), **MLDG** (Li et al. 2018), **F3-Net** (Qian et al. 2020), **LTW** (Sun et al. 2021), **MTA** (Zhao et al. 2021), **Local-relation** (Chen et al. 2021) and **GFF** (Luo et al. 2021).

The results in Tab. 1 show that our proposed DCL can significantly outperform the baseline model by around 5% on average and obtain the state-of-the-art performance compared with recently general face forgery detection methods, especially on Celeb-DF. Compared with other cross-entropy loss based methods, our two contrastive losses can both diversify the intra-category invariance and enhance the inconsistency of forgery face, thus the generalization can be improved significantly. In addition, the intra-domain performance(test on FF++) is better than the baseline model and

Method	GID-DF (HQ)		GID-DF (LQ)		GID-F2F (HQ)		GID-F2F (LQ)	
	ACC	AUC	ACC	AUC	ACC	AUC	ACC	AUC
EfficientNet	82.40	91.11	67.60	75.30	63.32	80.1	61.41	67.40
Focalloss	81.33	90.31	67.47	74.95	60.80	79.80	61.00	67.21
ForensicTransfer	72.01	-	68.20	-	64.50	-	55.00	-
Multi-task	70.30	-	66.76	-	58.74	-	56.50	-
MLDG	84.21	91.82	67.15	73.12	63.46	77.10	58.12	61.70
LTW	85.60	92.70	69.15	75.60	65.60	80.20	65.70	72.40
Ours	87.70	94.9	75.90	83.82	68.40	82.93	67.85	75.07

Table 4: Performance on multi-source manipulation evaluation, the protocols and results are from (Sun et al. 2021). GID-DF means training on the other three manipulated methods of FF++ and test on deepfakes class. The same for the others.

Inter	Views	Hard	Intra	Celeb-DF	DFD
	✓			74.12	88.32
✓				76.81	88.03
✓	✓			79.34	89.24
✓		✓		78.84	89.89
✓	✓	✓		80.30	90.12
✓	✓	✓	✓	82.30	91.66

Table 5: Ablation study on the influence of different components. Specifically, “Inter” means inter-instance contrastive learning module, “views” represents our special designed data views generation strategy, “hard” indicate the hard sample generation, and “Intra” is short for the Intra-instance contrastive learning module.

close to the local-relation (drop 0.16%), while our DCL outperforms it by over 2% on average in terms of AUC in unseen domain scenarios. To further demonstrate the robustness of our method, we also evaluate the generalization when testing on low-quality images. Concretely, follow the setting of (Masi et al. 2020), we train our model on FF++ (LQ) and test it on Deepfakes class and Celeb-DF. The quantitative results are shown in Tab. 2, we can observe that our method obtain state-of-the-art performance especially in a cross-database setting. The DCL outperforms by 5% compared with the recent SPSL and GFF on Celeb-DF and gets slight improvement on the intra-domain setting.

Cross-manipulation evaluation. To further demonstrate the generalization among different manipulated methods, we conduct this experiment on the FF++(HQ) dataset. We train a model on one method of FF++ and test it on all four methods. For a fair comparison, we reimplement Multi-attentional and GFF with EfficientNet-b4 as backbones.

As shown in Tab. 3, our DCL outperforms the competitors in most cases, including both intra-manipulation (Diagonal of the table) results and cross-manipulation. Specifically, when the train on Deepfakes and test on Faceswap, our DCL achieves over 15% performance gain on average in terms of AUC. Since different manipulation leaves different traces of forgery, a generalization model should find essential differ-

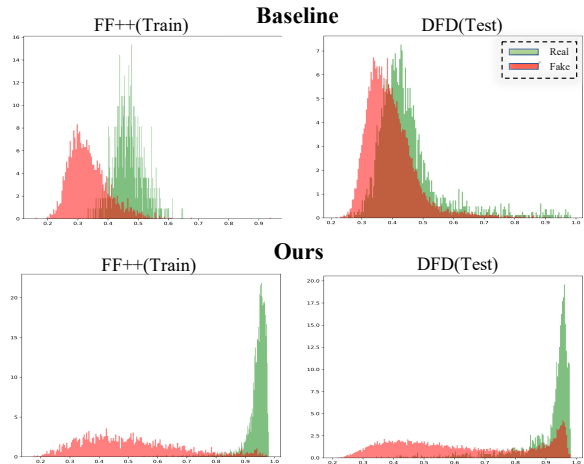


Figure 2: Histogram of the average of self-similarity for intra-domain dataset (FF++) and unseen domain (DFD). The first row indicates the histogram of the baseline model (En-b4) while the second row represents that of our DCL.

ences between real and fake faces. Our method carefully designed this difference in inter-instance contrastive learning module and hard sample generation strategy, thus improving the cross-manipulation performance.

Multi-source manipulation evaluation. In real-world applications, we usually have different manipulations samples to train while test on the unknown methods. We call these scenarios *Multisource cross-manipulation*. To demonstrate the practicality of our method, we conduct experiments based on the benchmarks build by (Sun et al. 2021) and change our backbone to EfficientNet-b0 for a fair comparison. The results are reported in Tab. 4. Our DCL obtains state-of-the-art performance on all protocols in terms of AUC and ACC. In particular, our method outperforms by the recent LTW around 5% on the low-quality version of FF++, which shows our method can guarantee generalization under different conditions and further demonstrates the robustness of our framework.

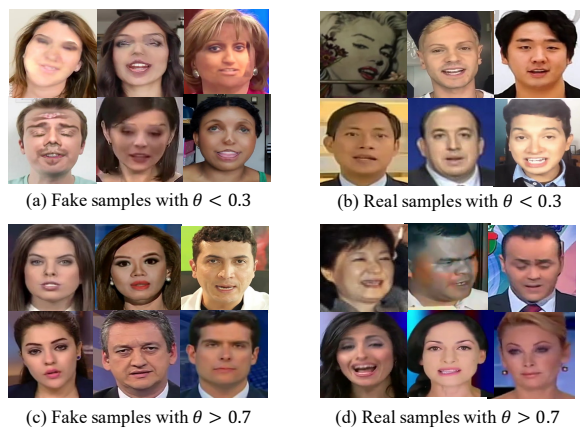


Figure 3: Visualization of the hard sample strategy with low and high threshold.

4.3 Ablation Study

To further explore the impact of different components of the DCL module, we split each part separately for verification. Specifically, we develop the following variants: 1) baseline model with our specially designed data views generation. 2) baseline model with common data augmentation and Inter-ICL without hard sample selection scheme. 3) DCL without hard sample generation. 4) DCL without specially designed data views generation. 5) DCL without Inter-ICL.

The quantitative results on Celeb-DF and DFD are reported in Tab. 5, the metric is AUC. The comparison between variant 2 and variant 3 can demonstrate the effectiveness of our specially designed data view transformation. The performance is further improved by 5% on Celeb-DF dataset when using Inter-ICL, which shows the importance of feature distributions for generalization. In addition, the hard sample selection scheme can bring around 1% improvement on both two datasets. In particular, the performance boosts significantly after adding Intra-ICL, demonstrating the efficiency of mining the inconsistency within the instance. Combining all the proposed components can achieve the best performance.

4.4 Visualization

Visualization of self-similarity. As shown in Fig. 2, we draw the histogram of the real and fake self-similarity on the baseline model and DCL to prove the effectiveness of our Intra-ICL. Specifically, we first train the DCL on FF++ (HQ), then the summation of self-similarity maps calculated by gram matrices is counted during the inference period. We can observe that the self-similarity of the baseline model lacks discriminative without additional constraints, while ours can be significantly separated in both intra-domain and unseen domain scenarios because of the Intra-ICL module.

Visualization of hard sample. Fig. 3 represents the fake and real samples filtered by our hard sample selection strategy. We contrast the feature with the prototypes which is orthogonal to the original class and use threshold θ to select samples. We can observe that the selection of fake sam-

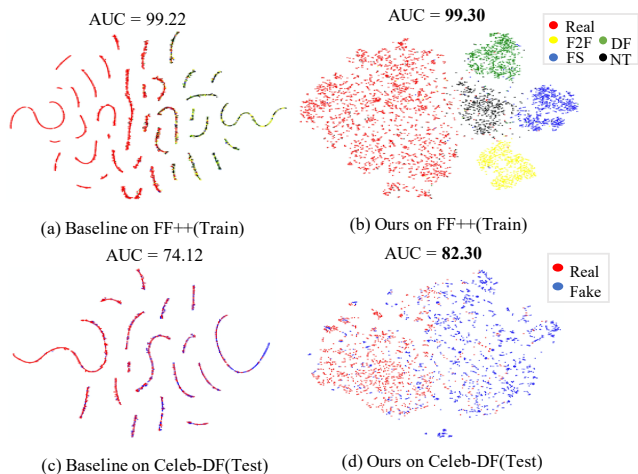


Figure 4: Feature distribution of baseline model (En-b4) and DCL on the intra-domain dataset (FF++) and unseen domain dataset (Celeb-DF) via t-SNE.

ples ($\theta > 0.7$) are relatively high-quality compared with low threshold samples, which cannot be easily distinguished. These samples always contain more essential forgery clues which are commonly presented under forgery faces. For real faces, the selected samples usually have abnormal expressions or heavy makeup which is easy to confuse with the fake face. And our framework takes these “hard” samples as negative pairs to promote mining the essential forgery clues.

Visualization of feature distribution. Our Inter-Contrastive learning aims to preserve the variations by avoiding clustering of same class features. To verify this phenomenon, we draw feature distribution of cross-entropy and DCL based model using t-SNE (Van der Maaten and Hinton 2008) technique. The visualization results are shown in Fig. 4. We can observe that the feature distributions of the same class are more dispersion than the baseline model and different manipulated methods are more separable, which improve the AUC of the unseen domain from 74.12% to 82.30%. This experiment demonstrates that the traditional supervised loss weakens the transferability due to the intra-category invariance, while our proposed DCL can improve the generalization by diverging the feature distribution.

5 Conclusion

In this work, we propose a holistic learning framework, named Dual Contrastive Learning (DCL) for general face forgery detection. Specifically, we generate data views via specially designed data transformations as positive pairs and propose Inter-instance Contrastive Learning (Inter-ICL) and Intra-instance Contrastive Learning (Intra-ICL) to mine the association among instances and inconsistency within each sample. In addition, we also introduce the hard sample selection strategy to select informative hard negative samples and brings further advantage to DCL. Experiments on three settings demonstrate the significant superiority of our method over state-of-the-art methods.

Acknowledgments

This work is supported by the National Science Fund for Distinguished Young Scholars (No.62025603), the National Natural Science Foundation of China (No.U1705262, No. 62072386, No. 62072387, No. 62072389, No. 62002305, No.61772443, No.61802324 and No.61702136), Guangdong Basic and Applied Basic Research Foundation(No.2019B1515120049), the Natural Science Foundation of Fujian Province of China (No.2021J01002), and the Fundamental Research Funds for the central universities (No. 20720200077, No. 20720200090 and No. 20720200091).

References

- Afchar, D.; Nozick, V.; Yamagishi, J.; and Echizen, I. 2018. Mesonet: a compact facial video forgery detection network. In *WIFS*, 1–7. IEEE.
- Bukchin, G.; Schwartz, E.; Saenko, K.; Shahar, O.; Feris, R.; Giryes, R.; and Karlinsky, L. 2021. Fine-grained Angular Contrastive Learning with Coarse Labels. In *CVPR*, 8730–8740.
- Chen, S.; Yao, T.; Chen, Y.; Ding, S.; Li, J.; and Ji, R. 2021. Local Relation Learning for Face Forgery Detection. *AAAI*.
- Chollet, F. 2017. Xception: Deep learning with depthwise separable convolutions. In *CVPR*, 1251–1258.
- Deng, J.; Dong, W.; Socher, R.; Li, L.-J.; Li, K.; and Fei-Fei, L. 2009. Imagenet: A large-scale hierarchical image database. In *CVPR*, 248–255. Ieee.
- Dolhansky, B.; Bitton, J.; Pflaum, B.; Lu, J.; Howes, R.; Wang, M.; and Ferrer, C. C. 2020. The DeepFake Detection Challenge Dataset. *arXiv preprint arXiv:2006.07397*.
- Frank, J.; Eisenhofer, T.; Schönherr, L.; Fischer, A.; Kolossa, D.; and Holz, T. 2020. Leveraging frequency analysis for deep fake image recognition. In *International Conference on Machine Learning*, 3247–3258. PMLR.
- Fridrich, J.; and Kodovsky, J. 2012. Rich models for steganalysis of digital images. *IEEE Transactions on Information Forensics and Security*, 7(3): 868–882.
- Gu, Z.; Chen, Y.; Yao, T.; Ding, S.; Li, J.; Huang, F.; and Ma, L. 2021. Spatiotemporal Inconsistency Learning for Deep-Fake Video Detection. In *Proceedings of the 29th ACM International Conference on Multimedia*, 3473–3481.
- Gutmann, M.; and Hyvärinen, A. 2010. Noise-contrastive estimation: A new estimation principle for unnormalized statistical models. In *Proceedings of the thirteenth international conference on artificial intelligence and statistics*, 297–304. JMLR Workshop and Conference Proceedings.
- He, K.; Fan, H.; Wu, Y.; Xie, S.; and Girshick, R. 2020. Momentum contrast for unsupervised visual representation learning. In *CVPR*, 9729–9738.
- Khosla, P.; Teterwak, P.; Wang, C.; Sarna, A.; Tian, Y.; Isola, P.; Maschinot, A.; Liu, C.; and Krishnan, D. 2020. Supervised contrastive learning. *arXiv preprint arXiv:2004.11362*.
- Li, D.; Yang, Y.; Song, Y.-Z.; and Hospedales, T. M. 2018. Learning to generalize: Meta-learning for domain generalization. In *AAAI*.
- Li, J.; Wang, Y.; Wang, C.; Tai, Y.; Qian, J.; Yang, J.; Wang, C.; Li, J.; and Huang, F. 2019a. DSFD: dual shot face detector. In *CVPR*, 5060–5069.
- Li, L.; Bao, J.; Zhang, T.; Yang, H.; Chen, D.; Wen, F.; and Guo, B. 2020. Face x-ray for more general face forgery detection. In *CVPR*, 5001–5010.
- Li, Y.; Chang, M.-C.; and Lyu, S. 2018. In Ictu Oculi: Exposing AI Created Fake Videos by Detecting Eye Blinking. *2018 IEEE International Workshop on Information Forensics and Security (WIFS)*, 1–7.
- Li, Y.; Yang, X.; Sun, P.; Qi, H.; and Lyu, S. 2019b. Celebdf: A new dataset for deepfake forensics. *arXiv preprint arXiv:1909.12962*.
- Liu, H.; Li, X.; Zhou, W.; Chen, Y.; He, Y.; Xue, H.; Zhang, W.; and Yu, N. 2021a. Spatial-phase shallow learning: rethinking face forgery detection in frequency domain. In *CVPR*, 772–781.
- Liu, S.; Zhang, K.-Y.; Yao, T.; Sheng, K.; Ding, S.; Tai, Y.; Li, J.; Xie, Y.; and Ma, L. 2021b. Dual reweighting domain generalization for face presentation attack detection. *IJCAI*.
- Lo, Y.-C.; Chang, C.-C.; Chiu, H.-C.; Huang, Y.-H.; Chen, C.-P.; Chang, Y.-L.; and Jou, K. 2021. CLCC: Contrastive Learning for Color Constancy. In *CVPR*, 8053–8063.
- Luo, Y.; Zhang, Y.; Yan, J.; and Liu, W. 2021. Generalizing Face Forgery Detection with High-frequency Features. In *CVPR*, 16317–16326.
- Masi, I.; Killekar, A.; Mascarenhas, R. M.; Gurudatt, S. P.; and AbdAlmageed, W. 2020. Two-branch recurrent network for isolating deepfakes in videos. In *ECCV*, 667–684. Springer.
- Matern, F.; Riess, C.; and Stamminger, M. 2019. Exploiting visual artifacts to expose deepfakes and face manipulations. In *WACVW*, 83–92. IEEE.
- Qian, Y.; Yin, G.; Sheng, L.; Chen, Z.; and Shao, J. 2020. Thinking in Frequency: Face Forgery Detection by Mining Frequency-aware Clues. In *ECCV*, 86–103. Springer.
- Robinson, J.; Chuang, C.-Y.; Sra, S.; and Jegelka, S. 2021. Contrastive learning with hard negative samples. *ICLR*.
- Rossler, A.; Cozzolino, D.; Verdoliva, L.; Riess, C.; Thies, J.; and Nießner, M. 2019. Faceforensics++: Learning to detect manipulated facial images. In *ICCV*, 1–11.
- Stehouwer, J.; Dang, H.; Liu, F.; Liu, X.; and Jain, A. 2019. On the detection of digital face manipulation. *arXiv preprint arXiv:1910.01717*.
- Sun, K.; Liu, H.; Ye, Q.; Liu, J.; Gao, Y.; Shao, L.; and Ji, R. 2021. Domain General Face Forgery Detection by Learning to Weight. In *AAAI*, volume 35, 2638–2646.
- Tan, M.; and Le, Q. V. 2019. Efficientnet: Rethinking model scaling for convolutional neural networks. *ICML*.
- Thies, J.; Zollhöfer, M.; Nießner, M.; Valgaerts, L.; Stamminger, M.; and Theobalt, C. 2015. Real-time expression transfer for facial reenactment. *ACM Trans. Graph.*, 34(6): 183–1.

Van der Maaten, L.; and Hinton, G. 2008. Visualizing data using t-SNE. *Journal of machine learning research*, 9(11).

Wang, T.; and Isola, P. 2020. Understanding contrastive representation learning through alignment and uniformity on the hypersphere. In *ICML*, 9929–9939. PMLR.

Wang, W.; Zhou, T.; Yu, F.; Dai, J.; Konukoglu, E.; and Van Gool, L. 2021. Exploring cross-image pixel contrast for semantic segmentation. *arXiv preprint arXiv:2101.11939*.

Wang, X.; Yao, T.; Ding, S.; and Ma, L. 2020. Face manipulation detection via auxiliary supervision. In *International Conference on Neural Information Processing*, 313–324. Springer.

Yang, X.; Li, Y.; and Lyu, S. 2019. Exposing deep fakes using inconsistent head poses. In *ICASSP*, 8261–8265. IEEE.

Zhao, H.; Zhou, W.; Chen, D.; Wei, T.; Zhang, W.; and Yu, N. 2021. Multi-attentional Deepfake Detection. *CVPR*.

Zhao, N.; Wu, Z.; Lau, R. W.; and Lin, S. 2020. What makes instance discrimination good for transfer learning? *ICLR*.

Zi, B.; Chang, M.; Chen, J.; Ma, X.; and Jiang, Y.-G. 2020. Wilddeepfake: A challenging real-world dataset for deepfake detection. In *ACM MM*, 2382–2390.